The rapidity dependence of the proton-to-pion ratio in Au+Au and p+p collisions at $\sqrt{s_{NN}}$ = 62.4 GeV and 200 GeV

I. G. Arsene[l], I. G. Bearden[f], D. Beavis[a], S. Bekele[k], C. Besliu[j], B. Budick[e], H. Bøggild[f], C. Chasman[a], C. H. Christensen[f], P. Christiansen[f], H. H. Dalsgaard[f], R. Debbe[a], J. J. Gaardhøje[f], K. Hagel[h], H. Ito[a], A. Jipa[j], E. B. Johnson[k], C. E. Jørgensen[f], R. Karabowicz[g], N. Katryńska[g], E. J. Kim[a,k], T. M. Larsen[l], J. H. Lee[a], G. Løvhøiden[l], Z. Majka[g], A. Marcinek[g], M. J. Murray[h,k], J. Natowitz[h], B. S. Nielsen[f], C. Nygaard[f], D. Pal[k], A. Oviller[l], R. Płaneta[g], F. Rami[b], C. Ristea[f], O. Ristea[j], D. Röhrich[i], S. J. Sanders[k], P. Staszel[g,1], T. S. Tveter[l], F. Videbæk[a,2], R. Wada[h], H. Yang[i], Z. Yin[i], I. S. Zgura[j], and V. Zhukova[k]

[a] *Brookhaven National Laboratory, Upton, New York 11973*
[b] *Institut de Recherches Subatomiques and Université Louis Pasteur, Strasbourg, France*
[c] *Institute of Nuclear Physics, Krakow, Poland*
[d] *Johns Hopkins University, Baltimore 21218*
[e] *New York University, New York 10003*
[f] *Niels Bohr Institute, Blegdamsvej 17, University of Copenhagen, Copenhagen 2100, Denmark*
[g] *Smoluchowski Inst. of Physics, Jagiellonian University, Kraków, Poland*
[h] *Texas A&M University, College Station, Texas, 17843*
[i] *University of Bergen, Department of Physics and Technology, Bergen, Norway*
[j] *University of Bucharest, Romania*
[k] *University of Kansas, Lawerence, Kansas 66045*
[l] *University of Oslo, Dep. of Physics, P.b. 1048 Blindern, 0316 Oslo, Norway*

Abstract

The proton-to-pion ratios measured with the BRAHMS spectrometers in Au+Au and p+p collisions at $\sqrt{s_{NN}}$ = 62.4 GeV and $\sqrt{s_{NN}}$ = 200 GeV, are presented as a function of transverse momentum and collision centrality at pseudo-rapidity values that range from 0 to 3.8. A strong pseudo-rapidity dependence of these ratios has been observed. The ratios measured in Au+Au collisions at $\sqrt{s_{NN}}$ = 200 GeV are compared to ratios calculated with models which incorporate hydro-dynamics, hadron rescattering and jet production. We compare the magnitude and p_T dependence of the p/π^+ratios measured in Au+Au collisions at $\sqrt{s_{NN}}$ = 200 GeV and $\eta \approx 2.2$, with the same ratio measured at $\sqrt{s_{NN}}$ = 62.4 GeV and $\eta = 0$. The striking agreement found between these ratios throughout the whole p_T range (up to 2.2 GeV/c) is consistent with particle production in A+A collisions being described with grand-canonical distributions, characterized by the baryo-chemical potential μ_B. At collision energy of 62.4 GeV and forward pseudo-rapidity we found a crossing point **in pseudo-rapidity for the p/π^+ ratio measured in central, semi-peripheral Au+Au as well as p+p reactions. The crossing occurs in a narrow η bin around 3.2 where all above listed systesms have the same p_T dependence.**

Key words: heavy ion collision, particle ratios, forward rapidity, hadronization
PACS: 25.75.q, 25.75.Dw, 25.40.-h, 13.75.-n

1. Introduction

The ongoing dialogue between theory and experiment is delivering a more clear picture of the QCD phase diagram in its partonic and hadronic phases. In particular, recent mid-rapidity RHIC results are considered as evidence for a smooth cross over from a dense and opaque partonic phase into a hadronic gas at temperatures around 170 MeV and small values of baryo-chemical potential μ_B [1].

Measurements of hadronic species abundances constrain statistical models used to describe the chemical freeze-out in nucleus-nucleus interactions at different energies. Some such models show a remarkable be-

[1] Corresponding author. Email: ufstasze@if.uj.edu.pl
[2] Spokesperson

havior at low baryo-chemical potential where the curves representing chemical freeze-out tend to merge with the phase boundary between partonic and hadronic media [2]. In such a picture, hadrons are produced very close to freeze-out, and one could safely state that the features of the partonic medium are transmitted to the final bulk hadrons via hadronization processes.

Indeed, such appears to be the case for the constituent quark scaling of elliptic flow v_2 measurements [3] as well as the enhancement of baryon-to-meson ratios that scale with the size of the created systems around mid-rapidity (low μ_B) [4, 6]. The observation of high baryon-to-meson ratios (≈ 1 for the so called intermediate p_T values ranging from 2 to 6 GeV/c) reported by the RHIC PHENIX collaboration [7] is inconsistent with pQCD predictions that include parton fragmentation in vacuum (extracted from $e^+ + e^-$ annihilations).

The measured p_T dependence of the baryon-to-meson ratio appears to be related to modifications in the hadronization mechanisms as it happens in a partonic medium. It was pointed out that the baryon-to-meson ratio p_T dependence should be sensitive to the hadronization scenario due to the different quark content of baryons and mesons and/or to radial flow of the bulk medium because of significant differences in baryon and meson masses. Both flow and medium quark coalescence are expected to enhance protons over pions at intermediate p_T.

The PHENIX $\bar{p}/\pi^-$ data at mid-rapidity is well described by the Greco, Ko, and Levai quark coalescence model [8] where the introduced coalescence involves partons from the medium (thermal) and partons from mini-jets. The Hwa and Yang quark recombination model is also successful in describing BRAHMS and PHENIX mid-rapidity data for p/π^+ [9]. On the other hand, the comparison with the hydrodynamical model shows that hydro-flow cannot itself account for the large observed ratio above ≈ 3 GeV/c and that the model overpredicts the data at low p_T [4]. These results support the view of a hadronization process driven by parton recombination with negligible final state interactions between produced hadrons. Nevertheless, at large μ_B, a significant gap between the temperature of the transition from the partonic to the hadronic phase, T_c, and the temperature of chemical freeze-out is predicted by QCD lattice calculation [5]. Thus at large μ_B, the picture, suggested by mid-rapidity measurements, might be contaminated by final state hadron interactions leading to a transition from the parton recombination scheme to a hydrodynamical description that has a common velocity field for baryons and mesons [10, 11].

2. Experimental setup

The BRAHMS detector setup [12] consists of two movable, small acceptance spectrometers: the Mid-Rapidity Spectrometer (MRS) which operates in the polar angle interval from $90^\circ \leq \Theta \leq 30^\circ$ (corresponding to a pseudo-rapidity interval of $0 \leq \eta \leq 1.3$) and the Forward Spectrometer (FS) which operates in the range from $2.3^\circ \leq \Theta \leq 15^\circ$ ($2 \leq \eta \leq 4$). The BRAHMS setup also includes detectors used to determine global features of the collision such as the overall charged particle multiplicity, collision vertex and the centrality of the collision. The MRS is composed of a single dipole magnet (D5) placed between two Time Projection Chambers (TPC) which provide a momentum mesurement. Particle identification (PID) is based on Time-of-Flight (TOF) measurements [12]. The FS spectrometer has two TPCs (which are capable of track recognition in a high multiplicity environment) close to the interaction region, and, at the far end of the spectrometer - three Drift Chambers (DC). **In the aggregate, the spectrometer can detect particle track segments with high momentum resolution ($\Delta p/p = 0.0008p$ at the highest field settings) using three dipole magnets.** Particle identification in the FS is provided by TOF measurements for low (H1) and medium (H2) particle momenta. High momentum particles are identified using a Ring Imaging Cherenkov detector (RICH) [13].

3. The analysis

The analysis reported in this letter consists of the comparison of proton and pions yields as function of p_T at several pseudo-rapidity intervals. Nominally, the BRAHMS spectrometers provide coverage to measure identified particle from $\eta = 0$ to $\eta = 3.8$. **The analysis method utilizes the feature of the same pion and proton acceptance in the η versus p_T space in the same real time measurement.** For a given η-p_T bin the p/π ratios are calculated on a setting by setting basis. In order to avoid mixing different PID techniques, which usually lead to different systematic uncertainties, the ratios are calculated separately for the TOF PID and the RICH PID. In this way, all factors such as acceptance corrections, tracking efficiencies, trigger normalization and bias related to the centrality cut cancel out in the ratio. The only remaining corrections are those that are species related which are:

(i) decay in flight, interaction with the beam pipe and the detector material budget,
(ii) the PID efficiency correction.

$\eta \approx 2.27$		$\eta \approx 2.65$		$\eta \approx 3.04$		$\eta \approx 3.3$		$\eta \approx 3.5$		$\eta \approx 3.7$	
p_T	p/π^+	p_T	p/π^+	p_T	p/π^+	p_T	p/π^+	p_T	p/π^+	p_T	p/π^+
0.5-0.8	< 1	0.5-0.7	< 2	0.4-0.6	< 3	0.3	3	0.3	3	0.4	**5**
1.0	2	0.9	2	0.8	**4.5**	0.45	4	0.4	6	0.5	**3.5**
1.2	3	1.15	3	0.9	**2**	0.6	6	0.55	**4**	0.6	**2**
1.6	**5**	1.2	**4**	1.1-2.0	$<$ **1**	0.7-2.0	$<$ **2**	0.7-1.7	$<$ **3**	> 0.75	$<$ **2**
> 1.7	$<$ **1**	> 1.3	$<$ **1**	> 2.2	**4**	3.0	6	2	**4**		
p_T	$\bar{p}/\pi^-$	p_T	$\bar{p}/\pi^-$	p_T	$\bar{p}/\pi^-$	p_T	$\bar{p}/\pi^-$	p_T	$\bar{p}/\pi^-$	p_T	$\bar{p}/\pi^-$
0.5-0.8	< 1	0.5-0.7	< 2	0.4-0.6	< 3	0.3	3	0.3	3	0.4	**14**
1.0	2	0.9	2	0.7	5	0.45	4	0.4	6	0.5	**11**
1.2	3	1.15	5	0.8	**6**	0.6	7	0.55	**12**	0.6	**8**
1.6	**5**	1.2	**3**	0.9	**4**	0.7	**7**	0.7	**7**	0.85	**5**
1.7	**2**	1.3	**2**	1.15-2.2	**3**	0.9-2.0	$<$ **3**	1.0-1.7	$<$ **4**	1.0	**3**
> 2.0	$<$ **1**	> 1.7	$<$ **1**	> 2.2	**4**	3.0	**6**	2.0	**4**	> 1.2	$<$ **2**

Table 1: Estimated PID systematic errors shown as a per-cent of the measured p/π^+ and $\bar{p}/\pi^-$ ratios presented in this letter. Regular and bold fonts refer to PID based on time-of-flight and Cherenkov measurement techniques, respectively.

The corrections for (i) are determined with events produced by the HIJING heavy-ion event generator [14] which in turn, are the input to a realistic GEANT [15] model description of the BRAHMS experimental setup. The magnitude of this correction depends on particle momenta and the the spectrometers positions but do not exceed 6%**. We estimate that the overall systematic uncertainty related to this correction is at the level of** 2%**.**

The PID efficiency correction of (ii) is calculated in different fashion depending on the spectrometer and the p_T range. The TOF PID is done separately for small momentum bins by fitting a multi-Gaussian function to the experimental squared mass M^2 distribution and applying a $\pm 3\sigma$ cut to select a given particle type. For measurements done with the FS spectrometer in the momentum range where pions overlap with kaons, (usually above 3.5 GeV/c) the RICH detector can be used in veto mode to select kaons with momentum smaller than the kaon Cherenkov threshold which is about 9 GeV/c. This procedure leads to a relatively clean sample of pions with some contamination by kaons having spurious rings associated in the RICH counter. Together with the kaon - proton overlap at larger momenta, this contamination effect is a source of systematic errors which have been estimated and collected in Tab. 1 for the FS spectrometer. At mid-rapidity the systematic uncertainty reaches a value of 5% at $p_T > 2.5$ GeV/c due to a limited kaon to pion separation at large momenta.

The RICH PID is also based on the particle separation in the M^2 versus momentum space. The RICH provides direct proton identification above the proton threshold momentum which is about 15 GeV/c. However, an additional proton identification scheme is possible above the kaon threshold, at this momentum range a proton is associated with tracks having moment above the kaon threshold, but no RICH signal (veto mode). The veto proton yields are corrected for pion and kaon contamination due to a finite RICH inefficiency. The RICH inefficiency was determined by studying yields of tracks identified in the TOF detector as pions but having no ring associated in the RICH. This study can be done for low magnetic fields in the momentum range corresponding to a good kaon/pion separation in TOF. It is found that the pion inefficiency is equal to unity at the pion threshold ($\approx$ 2.3 GeV/c) and rapidly decreases at larger momenta reaching a constant value of about 3% around 4 GeV/c. The RICH inefficiency found for pions is then applied to kaons (and the other species) assuming that Cherenkov radiation depends only on the gamma factor of the particle. A more detailed description of the RICH inefficiency analysis is given in [16]. There are two sources of systematic uncertainties associated with the RICH PID, namely, the uncertainty on the RICH inefficiency estimated to be at the level of 10% and the overlap in M^2 between pions and kaons having momenta above about 30 GeV/c. The overall systematic errors on p/π^+ and $\bar{p}/\pi^-$ related to RICH PID measurement are summarized in Tab. 1 (in bold).

4. Results

It has already been shown that the p/π ratios in the intermediate p_T range depend very strongly on both the charge and the pseudo-rapidity of emitted particles, as well as on the size of colliding systems [4].

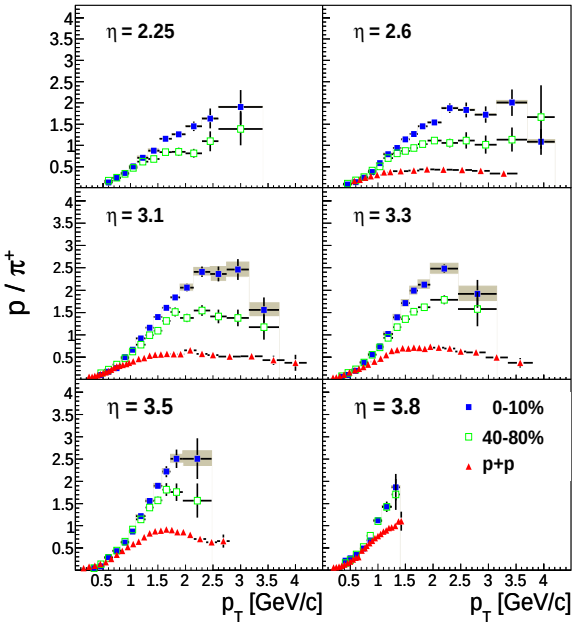

Figure 1: Centrality dependent p/π^+ ratio for Au+Au system colliding at $\sqrt{s_{NN}}$ = 200 GeV for central (0 – 10%) and semi-peripheral (40 – 80%) reactions in comparison with p+p collision data at the same energy. The vertical bars represent the statistical errors and the shaded boxes (plotted only for central Au+Au) show the systematic uncertainties.

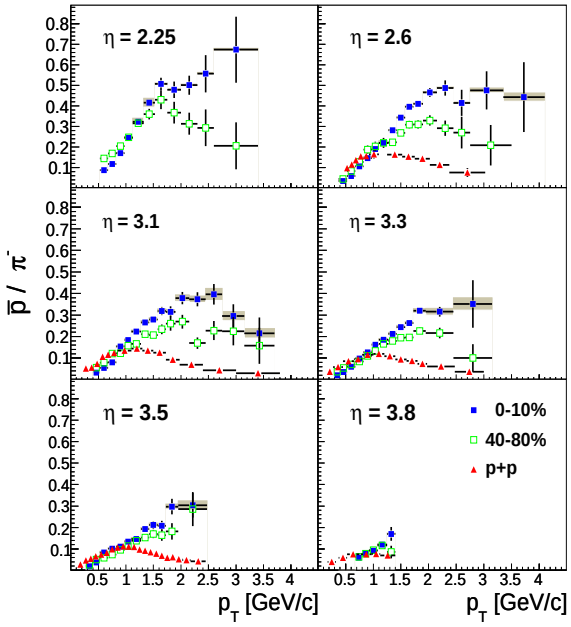

Figure 2: Same as Fig. 1 but here the ratios for negative changes, $\bar{p}/\pi^-$, are plotted.

Figure 1 shows p/π^+ ratios obtained for Au+Au reacting at $\sqrt{s_{NN}}$ = 200 GeV for two collision centrality classes of events, namely, for centrality 0 – 10% **(solid dots) and** 40 – 80% **(open squares). The centrality selection is based on charged-particles multiplicity in the range** $-2.2 < \eta < 2.2$ **as described in [17].** The shaded boxes, plotted for the most central events, represent the systematic uncertainties discussed in the previous section. The ratios extracted from p + p data at the same energy are plotted for comparison (solid triangles). The p_T coverage depends on the pseudo-rapidity bins and extends up to p_T = 4 GeV/c for η = 2.6 and 3.1. At low p_T (< 1.5 GeV/c) the p/π^+ ratios exhibit a rising trend with a weak dependence on centrality. The dependency on centrality begins above 1.5 GeV/c. The ratios appear to reach a maximum value at p_T around 2.5 GeV/c (whenever there is enough p_T coverage). The maxima of the ratios increase with the level of centrality and at η = 3.1, are equal to about 2.5 and 1.5 for the 0 – 10% and 40 – 80% centrality bins, respectively. The p+p ratios are consistent with Au+Au data at low p_T and begin to deviate significantly above p_T = 1 GeV/c. At η = 3.1 a maximum value of the ratio of 0.55 is reached in p+p collisions which is a factor of 4.5 smaller than that observed for central Au+Au reactions. **We performed PYTHIA calculations [18] for nucleon-nucleon interactions is each possible izospin state. These calculations have shown that the izospin has no impact on the discrepancy in p/π observed in Au+Au and p+p reactions.**

The values of the $\bar{p}/\pi^-$ ratios plotted in Fig. 2 are significantly lower than the p/π^+ ratios (note the difference in the vertical scale), however, the centrality dependence shows the same features as those observed in the p/π^+ ratios, namely, that the ratios for different centrality classes are consistent with each other up to $p_T \approx$ 1.2 GeV/c and a strong dependence on centrality appears at larger transverse momenta reaching a maxmimum at similar p_T as the positive particles. Looking at the p + p data alone, one notes the difference in shape between the p/π^+ and $\bar{p}/\pi^-$ ratios: a clear shift of the $\bar{p}/\pi^-$ peaks towards lower p_T , as well as a much broader p/π^+ peaks. The large difference between the Au+Au and p+p both in shape and overall magnitude may reflect significant medium effects in Au+Au at $\sqrt{s_{NN}}$ = 200 GeV in the pseudo-rapidity intervals covered.

An interesting picture is revealed at very low p_T in particular for $\bar{p}/\pi^-$ ratios which are plotted in Fig. 3 for central and semi-peripheral Au+Au and for p+p reactions at the same 200 GeV energy. Namely, below

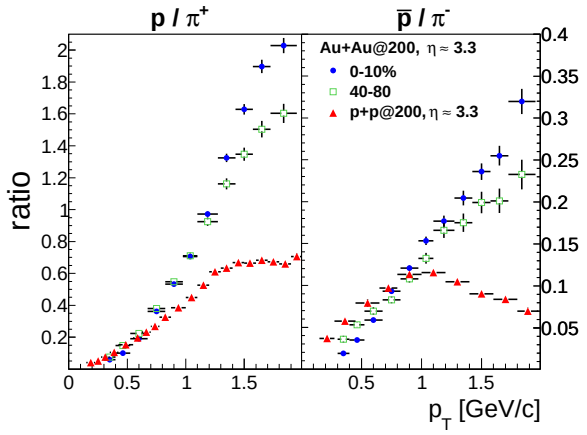

Figure 3: Centrality dependent p/π^+ (left) and $\bar{p}/\pi^-$ (right) ratio for Au+Au system colliding at $\sqrt{s_{NN}}$ = 200 GeV and for p+p collisions at the same energy. The data are limited to low p_T .

$\approx$ 0.9 GeV/c the $\bar{p}/\pi^-$ ratio increases towards more peripheral reactions and reaches the largest value for p+p reactions. Moreover, the ratios for Au+Au, for different centrality classes and for p+p cross each other at approximately the same point, located at about 0.9 GeV/c.

5. Model predictions

To interpret these results, theoretical models of nucleus-nucleus collisions are confronted with the data. The curves in Fig. 4 compare our results for 0 − 10% central Au+Au reactions at $\sqrt{s_{NN}}$ = 200 GeV to the THERMINATOR model [20] (black dashed lines) and AMPT model [21] (solid lines). The THERMINATOR is 1+1 D model that incorporates rapidity dependence of statistical particle production (including the excited states) imposed on the hydro-dynamical flow.

The AMPT (A Multi-Phase Parton Transport) is a rather complex model that includes mini-jet parton production, parton dynamics, hadronization according to the LUND string fragmentation model , and final state hadronic interactions. The p/π^+ ratio measured in central Au+Au collisions at $\sqrt{s_{NN}}$ = 200 GeV shown on the top row of Fig. 4 has a strong growth with rapidity; starting from a value of about 1.0 at $\eta \approx 0$ and $p_T \approx 3GeV/c$ and reaching a value of 2.5 at $\eta \approx 3.5$ and $p_T \approx 3GeV/c$. In contrast, the $\bar{p}/\pi^-$ ratio (bottom row) decreases with increasing rapidity (from $\approx$ 1 at $\eta \approx 0$ to 0.4 at $\eta \approx 3.5$). (Note the different vertical scales for positive and negative charged particles).

At forward rapidities the THERMINATOR model describes our data quite well up to $p_T \approx$ 2.5 GeV/c, both for ratios of positive and negative particles. For $\eta = 0$ this model underpredicts the experimental p/π^+ and $\bar{p}/\pi^-$ ratios in the intermediate p_T range covered by the data ($1 < p_T < 3$ GeV/c). At large p_T (> 3 GeV) THERMINATOR fails to describe the data. The mismatch is clearly seen in the $\eta = 3.05$ plot of Fig. 4 where the data have the best p_T coverage. This mismatch is attributed to the fact that the model does not include the production of jets. The AMPT model can qualitatively describe the pseudo-rapidity trends, but fails to quantitatively describe the data, namely, the model underpredicts p/π^+ and overpredicts $\bar{p}/\pi^-$ ratios. We also compared AMPT calculations with the low p_T data presented in Fig. 4. We note that the AMPT describes the p/π^+ ratios reasonably well for semi-peripheral reactions, however, it underpredicts the ratio for the most central collisions and significantly overpredicts p/π^+ ratio for p+p reactions. For the $\bar{p}/\pi^-$ data the AMPT model can predict the correct trend in the centrality dependence but the overall quantitative agreement with data is poor, e.g. the $\bar{p}/\pi^-$ for p+p reactions are overpredicted by a factor of 2. **In Fig. 5 we explore the possible connection between the measured p/π ratios in extended systems and the baryo-chemical μ_B used to characterize them as statistical systems. Such connection is done comparing the p/π^+ measured in Au+Au collisions at $\sqrt{s_{NN}}$ = 62.4 GeV and η = 0.0 shown with open red (on-line) triangles and the same ratio measured in Au+Au reactions at $\sqrt{s_{NN}}$ = 200 GeV and η = 2.2 shown with the black triangles. The pseudo-rapidity intervals selected for this comparison, namely η = 0.0 for Au+Au at $\sqrt{s_{NN}}$ = 62.4 GeV and η = 2.2 for Au+Au at $\sqrt{s_{NN}}$ = 200 GeV correspond to similar $\bar{p}/p$ = 0.45, which in turn, has been connected to a common value of the baryo-chemical potential μ_B of the observed bulk media, equal to $\approx$ 62 MeV for these two energies [22, 23]. The similarity of proton-to-pion ratios for these selected heavy ion collisions suggests that the baryon and meson production at the p_T interval studied (up to 2 GeV/c) is dominated by medium effects and is determined by the bulk medium properties. The considerably lower values of the p/π^+ ratio measured in the p+p system at $\sqrt{s}$ = 200 GeV, shown with grey stars in 5, can also be construed as strong indication that medium effects in nucleus-nucleus are the source of the observed enhancement of the p/π as function of p_T in the nucleus-nucleus collisions.** In addition, Fig. 5 shows that the THERMINATOR model calculations (dashed curve) describes central Au+Au data reasonably well.

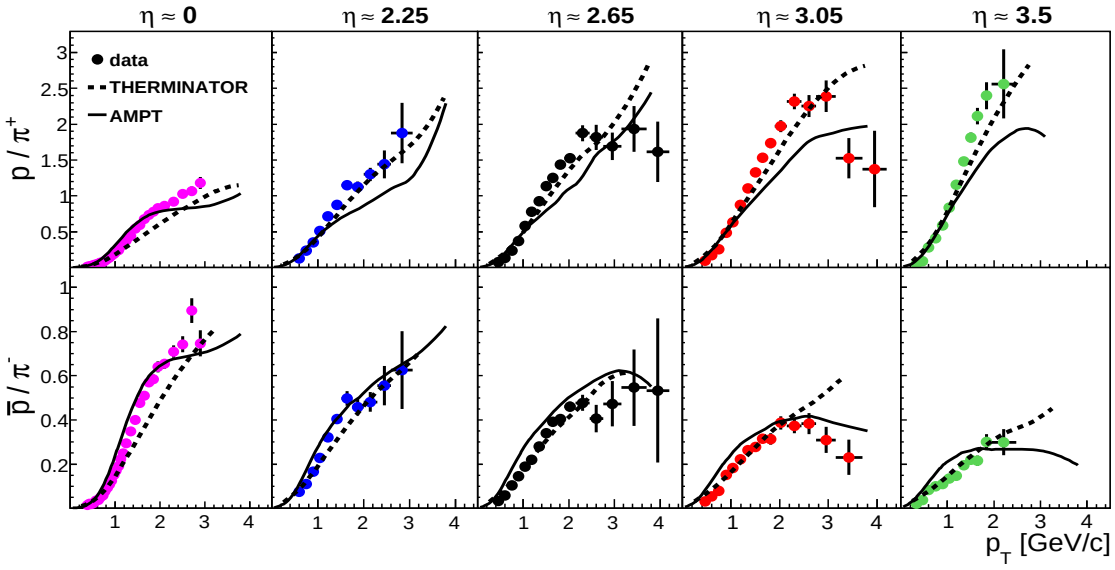

Figure 4: Forward region rapidity evolution of p/π^+ and $\bar{p}/\pi^-$ for 0 – 10% central Au+Au reaction at $\sqrt{s_{NN}}$ = 200 GeV (solid points), and predictions from the THERMINATOR model (dashed line) and hydrodynamic model (solid line).

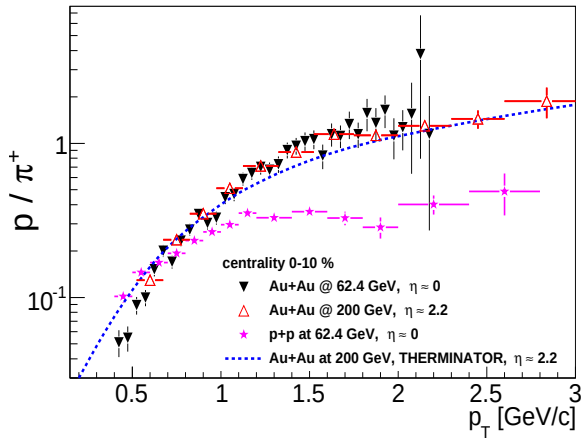

Figure 5: p/π^+ ratio in Au+Au collisions for η = 0.0 at $\sqrt{s_{NN}}$ = 62.4 GeV marked with open red (on-line) triangles and the Au+Au reactions for η = 2.2 at $\sqrt{s_{NN}}$ = 200 GeV marked with the black triangles. Dashed blue(on-line) curve shows description of central Au+Au collisions at $\sqrt{s_{NN}}$ = 200 GeV by the THERMINATOR code [20]. Stars (pink on line) shown reference mid-rapidity data for p+p at $\sqrt{s_{NN}}$ = 62.4 GeV.

6. Forward ratios at 62 GeV

The three panels of Fig. 6 display the p/π^+ ratio extracted from p+p and Au+Au collisions at $\sqrt{s_{NN}}$ = 62.4 GeV measured at 3 different pseudo-rapidity bins, namely η = 2.67 (top panel), η = 3.2 (middle panel) and η = 3.5 (bottom panel). The message we try to convey with this figure is the existence of a crossing point in pseudo-rapidity. On the low rapidity side of that point (top panel with η = 2.67) the p/π^+ ratio from central Au+Au reactions is greater with respect to the one from p+p collisions by a factor of 1.6. Whereas on the high rapidity side (lower panel with η = 3.5) the situation is reversed, namely, p/π^+ ratio in p+p exceeds the one measured in central Au+Au by a factor of about 1.4. The middle panel of 6 shows the p/π^+ ratios from Au+Au and p+p collisions at $\sqrt{s_{NN}}$ = 62.4 GeV at η = 3.2. This so called crossing point in pseudo-rapidity shows a remarkable complete overlap of the ratios as function of p_T not only for p+p and 0 – 10% central Au+Au reactions, but also for other Au+Au centralities, namely 10 – 20%, 20 – 40% and 40 – 80%. **Such universal shape of p/π^+ ratios implies that nuclear modification factor for protons and pions are consistent with each other at all p_T and all centrality at this pseudo-rapidity.** The observed crossing of p/π^+ ratios for different size of colliding systems is consistent with recent BRAHMS results on centrality dependence of net-proton rapidity distribution in Au+Au reactions at $\sqrt{s_{NN}}$ = 200 GeV [25]. The data show

an increased baryon transport towards mid-rapidity in central collisions. Such increased stopping power dissipates the longitudinal beam energy to form a denser system where recombination mechanisms favor proton production at intermediate values of p_T . Both effect will produce higher values of the p/π^+ ratio in extended systems. On the other hand, at very forward rapidities (around one unit below the beam rapidity) a bigger fraction of the measured particles are protons and their numbers are even higher for lighter systems due to reduced stopping power. Such observation is consistent with to the reversed p/π^+ dependency on the system size seen in the bottom panel. A crossing of p/π^+ ratios at energy of 62.4 GeV is predicted by UrQmd [26], HIJING and AMPT model calculations. However, these models predict the location of the crossing point in the interval $2 < y < 2.5$ *(how to refer to this?)*, which is almost one unit of rapidity lower than the observed value. These experimental results will then provides a strong constrain on the theoretical description of baryon number transport and associated energy dissipation in relativistic nuclear reactions. It is worth to notice, that for reactions at energy of 200 GeV (see Fig. 1), even at $\eta = 3.8$, the p/π^+ ratios measured in Au+Au reactions are larger than those observed in p+p, so the possible crossing point at high energy is located at larger rapidity, beyond the experimental acceptance.

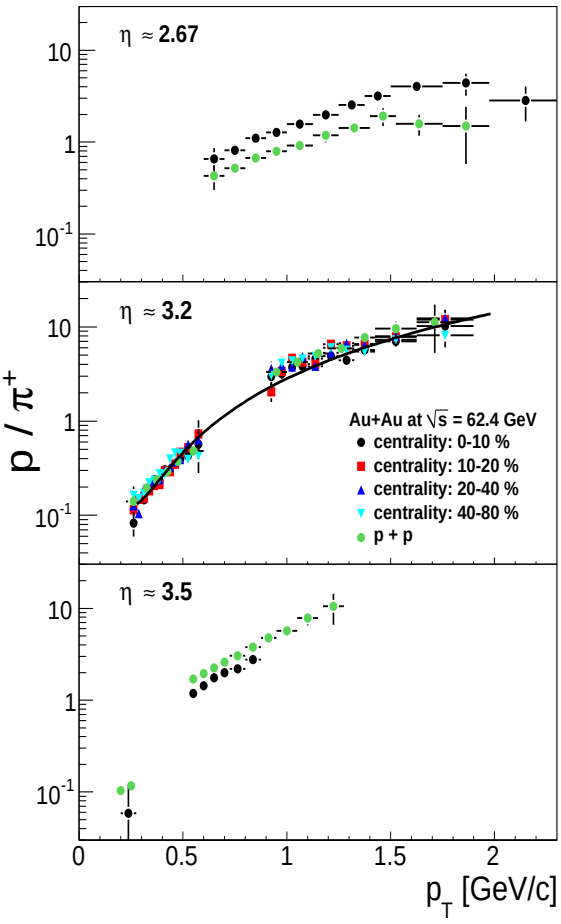

Figure 6: p/π^+ ratio from p+p and Au+Au collisions at $\sqrt{s_{NN}}$ = 62.4 GeV for $\eta = 2.67$ (top panel), $\eta = 3.2$ (middle panel) and $\eta = 3.5$ (bottom panel).

7. Summary and discussion

We presented the (p_T) dependence of the p/π ratios measured in Au+Au and p+p collisions at energies 62.4 and 200 GeV as a function of pseudo-rapidity and collision centrality (Au+Au). The data provide the opportunity to study baryon-to-meson production over a wide range of the baryo-chemical potential, μ_B. For Au+Au and p+p reactions at $\sqrt{s_{NN}} = 200$ GeV the p/π^+ and $\bar{p}/\pi^-$ ratios show noticeable dependency on centrality at intermediate p_T with a rising trend from p+p to central Au+Au collisions. We have shown that p/π^+ ratios are remarkably similar for central Au+Au at $\sqrt{s_{NN}} = 200$ GeV, $\eta \approx 2.2$ and central Au+Au at $\sqrt{s_{NN}} = 62.4$ GeV, $\eta \approx 0$, where the bulk medium is characterized by the same value of $\bar{p}/p$. This observation, together with the observed centrality dependence suggests, that at these energies and pseudo-rapidity intervals, particle production at intermediate p_T is governed by the size and chemical properties of the created medium. It was also shown that THERMINATOR, used as a reference model in our studies, underpredicts the p/π^+ and $\bar{p}/\pi^-$ ratios for central Au+Au at $\sqrt{s_{NN}} = 200$ GeV at mid-rapidity. This is, however, expected within the picture of hadronization process driven by parton coalescence followed by weak final interactions of hadrons that can not bring different hadronic species to the common local collective velocity field assumed in the model. On the other hand THERMINATOR provides good quantitative description of data at forward rapidity, namely from $\eta \approx 2.2$ to ≈ 3.5. This may indicate that in this domain, the final hadronic interactions take place long enough (before freeze-out) to suppress the relative collectivity of different species, which is a remnant effect of earlier hadronization via parton coalescence. Finally, the Au+Au and p+p measurements at $\sqrt{s_{NN}} = 62.4$ GeV show that the p/π^+ ratios for p+p and for all analysed Au+Au centralities cross simultaneously at the same η value (≈ 3.2) and are consistent with each other in the covered p_T range e.g. from 0.3 GeV/c up to 1.8 GeV/c.

This work was supported by the Division of Nuclear Physics of the Office of Science of the U.S. Department of Energy under contracts DE-AC02-98-CH10886, DE-FG03-93-ER40773, DE-FG03-96-ER40981, and DE-FG02-99-ER41121, the Danish Natural Science Research Council, the Research Council of Norway, the Polish Ministry of Science and Higher Education (Contract no 1248/B/H03/2009/36), and the Romanian Ministry of Education and Research (5003/1999, 6077/2000). We thank the staff of the Collider-Accelerator Division at BNL for their excellent and dedicated work to deploy RHIC and their support to the experiment.

References

[1] M. Stephanov, XXIV International Symposium on Lattice Field Theory, Tucson, Arizona, USA, July 23-28, 2006, Z. Fodor, arXiv:0712.2930v1 [hep-lat].
[2] P. Braun-Munzinger, Nucl. Phys. **A 681** 119c-123c (2001).
[3] R. A. Lacey, and A. Taranenko, The 2nd Edition of International Workshop - Correlations and Fluctuations in Relativistic Nuclear Collisions, Galileo Galilei Institute, Florence, Italy, July 7-9, 2006.
[4] E. J. Kim (BRAHMS Collaboration), Nucl. Phys. **A 774** 493-496 (2006).
[5] P. Braun-Munzinger, J. Stachel, Jour. of Phys. **G 28** 1971 (2002).
[6] R. Debbe, Quark Matter 2008, Jaipur, India, February 3-10, 2008, BRAHMS plenary talk.
[7] K. Adcox et. al., [PHENIX Collaboration], Phys. Rev. Lett. **88** 242301 (2002).
[8] V. Greco, C.M. Ko, and P. Levai, Phys. Rev. Lett. **90**022302 (2003).
[9] R. C. Hwa, and C. B. Yang, Phys. Rev. **C 67** 034902 (2003).
[10] T. Hirano, and Y. Nara, Nucl. Phys. **A743** 305 (2004).
[11] W. Broniowski, and W. Florkowski, Phys. Rev. Lett. **87** 272302 (2001).
[12] BRAHMS Collaboration, Nucl. Instr. Meth. **A 499** 437 (2003).
[13] R. Debbe et. al., Nucl. Instr. Meth. **A 570** 216 (2007).
[14] M. Gyulassy and X. N. Wang, Comput. Phys. Commun. **83** 307 (1994).
[15] "GEANT: Detector Description and Simulation Tool", wwwinfo.cern.ch/asdoc/geant_html3/
[16] BRAHMS Collaboration Long Paper (Phys. Rev D. in preparation).
[17] I.G. Bearden et. al. [BRAHMS Collaboration], Phys. Rev. Lett. **88** 202301 (2002).
[18] T. Sjostrand, Comp. Phys. Commun. **82**, 74 (1994), http://www.thep.lu.se/tf2/staff/torbjorn/Pythia.thml.
[19] T. Hirano, and Y. Nara, Phys. Rev **C 69**, 034908 (2004).
[20] W. Broniowski, and B. Biedroń, Phys. Rev. **C 75** 054905 (2007).
[21] Z. Lin, Phys. Rev. **C 72** 064901 (2005).
[22] I.G. Bearden et. al. [BRAHMS Collaboration], Phys. Rev. Lett. **90** 102301 (2003).
[23] I.C. Arsene et. al., for BRAHMS Collaboration, Int. Jour. of Mod. Phys.**E 16** 2035 (2007), I.C. Arsene [for the BRAHMS Collaboration], IJMPE **16**, (2007) 2035.
[24] R. C. Hwa, and C. B. Yang, Phys. Rev. **C 76** 014901 (2007).
[25] F. Videbaek, Quark Matter 2009, Knoxville, USA, April 2009, BRAHMS plenary talk.
[26] M. Bleicher et. al., J. Phys. G: Part. Phys. **25**, 1859 (1999).